JACS JOURNAL OF THE AMERICAN CHEMICAL SOCIETY
pubs.acs.org/JACS
Communication

A Thioether-Ligated Cupric Superoxide Model with Hydrogen Atom Abstraction Reactivity

Mayukh Bhadra, Wesley J. Transue, Hyeongtaek Lim, Ryan E. Cowley, Jung Yoon C. Lee, Maxime A. Siegler, Patrick Josephs, Gerald Henkel, Markus Lerch, Siegfried Schindler, Adam Neuba, Keith O. Hodgson, Britt Hedman, Edward I. Solomon,* and Kenneth D. Karlin*

Cite This: *J. Am. Chem. Soc.* 2021, 143, 3707−3713
Read Online

ACCESS | Metrics & More | Article Recommendations | Supporting Information

ABSTRACT: The central role of cupric superoxide intermediates proposed in hormone and neurotransmitter biosynthesis by noncoupled binuclear copper monooxygenases like dopamine-β-monooxygenase has drawn significant attention to the unusual methionine ligation of the Cu_M ("Cu_B") active site characteristic of this class of enzymes. The copper−sulfur interaction has proven critical for turnover, raising still-unresolved questions concerning Nature's selection of an oxidizable Met residue to facilitate C−H oxygenation. We describe herein a model for Cu_M, $[(^{\mathrm{TMG}}\mathrm{N}_3\mathrm{S})\mathrm{Cu}^{\mathrm{I}}]^+$ ($[\mathbf{1}]^+$), and its O_2-bound analog $[(^{\mathrm{TMG}}\mathrm{N}_3\mathrm{S})\mathrm{Cu}^{\mathrm{II}}(\mathrm{O}_2^{\bullet-})]^+$ ($[\mathbf{1}\cdot\mathrm{O}_2]^+$). The latter is the first reported cupric superoxide with an experimentally proven Cu−S bond which also possesses demonstrated hydrogen atom abstraction (HAA) reactivity. Introduction of O_2 to a precooled solution of the cuprous precursor $[\mathbf{1}]\mathrm{B}(\mathrm{C}_6\mathrm{F}_5)_4$ (−135 °C, 2-methyltetrahydrofuran (2-MeTHF)) reversibly forms $[\mathbf{1}\cdot\mathrm{O}_2]\mathrm{B}(\mathrm{C}_6\mathrm{F}_5)_4$ (UV/vis spectroscopy: $\lambda_{\max}$ 442, 642, 742 nm). Resonance Raman studies (413 nm) using $^{16}O_2$ [$^{18}O_2$] corroborated the identity of $[\mathbf{1}\cdot\mathrm{O}_2]^+$ by revealing Cu−O (446 [425] cm^{-1}) and O−O (1105 [1042] cm^{-1}) stretches, and extended X-ray absorption fine structure (EXAFS) spectroscopy showed a Cu−S interatomic distance of 2.55 Å. HAA reactivity between $[\mathbf{1}\cdot\mathrm{O}_2]^+$ and TEMPO−H proceeds rapidly (1.28×10^{-1} M^{-1} s^{-1}, −135 °C, 2-MeTHF) with a primary kinetic isotope effect of $k_H/k_D = 5.4$. Comparisons of the O_2-binding behavior and redox activity of $[\mathbf{1}]^+$ vs $[\mathbf{2}]^+$, the latter a close analog of $[\mathbf{1}]^+$ but with all N atom ligation (i.e., N_3S vs N_4), are presented.

The noncoupled binuclear (NCBN) copper monooxygenase family of peptidylglycine-α-hydroxylating monooxygenase (PHM), dopamine-β-monooxygenase (DβM), and tyramine-β-monooxygenase (TβM) is crucial to hormone and neurotransmitter biosynthesis. This family is characterized by two distant (11−14 Å) copper centers Cu_M (Cu_B) and Cu_H (Cu_A) (Figure 1). The former has a $MetHis_2$ coordination sphere and is thought to play the major role in O_2 activation and substrate-binding, while the latter has His_3 coordination and behaves as an electron relay.[1−4] After years of study,[2,5−10] experimental and computational evidence have mostly converged on an end-on (η^1) superoxide $Cu_M^{II}(O_2^{\bullet-})$ intermediate hypothesized as the active species in substrate hydrogen atom abstraction (HAA), initiating C−H hydroxylation.[11] Such an intermediate is distinct from other proposed cupric superoxides[12−14] due to the presence of an oxidizable methionine at Cu_M. In fact, this Met has proven critical to turnover, as mutants lacking sulfur ligation (Met, Cys) have been inactive.[15]

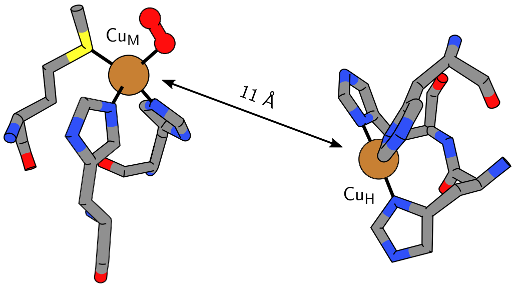

Figure 1. A depiction (PDB: 1SDW)[2] of the copper centers of PHM, the O_2-binding Cu_M, and the electron relay Cu_H.

The criticality of the methionine remains unexplained[16−19] prompting model system investigations. These have demonstrated the influences of denticity,[4,20−25] electron richness,[26,27] steric modulation,[28,29] coordination geometry,[30] temperature, solvent,[31] and hydrogen bonding[32,33] on electronic structure and reactivity.

Despite these insights, we still lack a $Cu^{II}O_2^{\bullet-}$ model with a clear Cu^{II}−S interaction and its corresponding HAA reactivity. Although thioether-containing tridentate or tetradentate ligand-copper models have been investigated,[34−41] many synthetic attempts rather form binuclear cupric peroxides,[37,42−44] and none exhibit substrate oxidative reactivity. Our recent report[45] using a modified TMPA ligand[26] succeeded in observation of a mononuclear $Cu^{II}O_2^{\bullet-}$ in the presence of a thioether; however, direct evidence of the Cu−S interaction by (EXAFS) spectroscopy eluded us. Furthermore,

Received: January 8, 2021
Published: March 8, 2021

https://dx.doi.org/10.1021/jacs.1c00260
J. Am. Chem. Soc. 2021, 143, 3707−3713

the extreme instability of this complex prevented rigorous spectroscopic and reactivity studies, as it rapidly formed the more stable *trans*-peroxide.

We now report that the $^{TMG}N_3S$ ligand[39] supports a cupric superoxide, $[(^{TMG}N_3S)Cu^{II}O_2^{\bullet -}]^+$ ($[\mathbf{1}\cdot O_2]^+$), with a demonstrable Cu^{II}−S interaction (Scheme 1) and HAA reactivity.

Scheme 1. Compound $[\mathbf{1}]B(C_6F_5)_4$ Reversibly Binds O_2 upon Cooling to −135 °C in 2-MeTHF, Forming $[\mathbf{1}\cdot O_2]B(C_6F_5)_4$

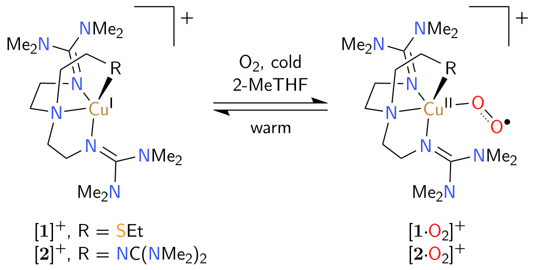

Resonance Raman (rR) studies confirmed the identity of ($[\mathbf{1}\cdot O_2]^+$) as a superoxide complex, and EXAFS studies demonstrate the first irrefutable Cu−S bond in a CuO_2 complex. Beyond the relevance of $[\mathbf{1}\cdot O_2]^+$ as an NCBN structural model with $Cu{-}S_{thioether}$ ligation, it is the first functional mimic of the Cu_M active site.

The O_2-chemistry of [**1**]OTf was previously interrogated, but no superoxide formation was observed in acetone at −76 °C.[39] However, the success of the similar TMG_3tren ligand in supporting a stabilized cupric superoxide $[\mathbf{2}\cdot O_2]^+$[28,46−48] encouraged our exploration of broader experimental conditions for the $-CH_2CH_2SEt$ ligand analog, $[\mathbf{1}\cdot O_2]^+$ (Scheme 1). We sought lower temperatures by a switch from acetone to 2-MeTHF, also requiring a switch to tetrakis(pentafluorophenyl)borate, $B(C_6F_5)_4^-$, as the counteranion. Combination of $^{TMG}N_3S$ with $[Cu^I(CH_3CN)_4](C_6F_5)_4$ in 2-MeTHF provided $[\mathbf{1}]B(C_6F_5)_4$ (87% yield) following workup and recrystallization. Our present single crystal X-ray diffraction (XRD) study (see Section 2 in the Supporting Information (SI)) revealed a monomeric species with a normal Cu−S distance of 2.2709(5) Å (Figure 2a).[37,39,42−44] $[\mathbf{1}]B(C_6F_5)_4$ possesses unremarkable Cu−N distances of 2.0362(15), 2.0436(15), and 2.1987(14) Å. This four-coordinate, distorted trigonal pyramidal geometry presents an open fifth coordination site for further ligand binding.

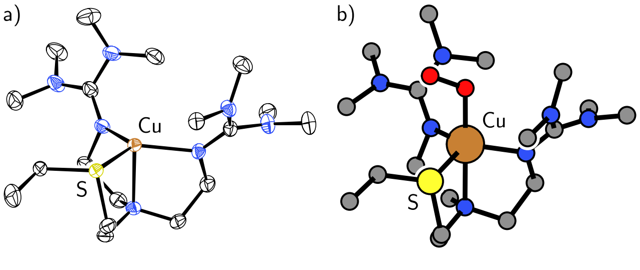

Figure 2. (a) Displacement ellipsoid plot (50% probability level) of $[\mathbf{1}]B(C_6F_5)_4$ at 110(2) K with a Cu−S distance of 2.2709(5) Å. Hydrogen atoms and counterions have been omitted for clarity. (b) Structure of $[\mathbf{1}\cdot O_2]^+$ from density functional theory (DFT) calculations. Selected interatomic distances [Å] and angles [deg]: Cu−S 2.50, Cu−O 1.99, O−O 1.29; Cu−O−O 113.0.

Exposure of a precooled solution of $[\mathbf{1}]B(C_6F_5)_4$ (0.39 mM, 2-MeTHF, −135 °C) to excess O_2 evinced the brilliant green color of $[\mathbf{1}\cdot O_2]B(C_6F_5)_4$. UV/vis spectroscopic monitoring (Figures S1 and S2) revealed growth of features at λ_{max} 442 nm (ε 3700 M^{-1} cm^{-1}), 642 nm (ε 1525 M^{-1} cm^{-1}), and 742 nm (ε 1675 M^{-1} cm^{-1}),[49] matching well with those of $[\mathbf{2}\cdot O_2]^+$.[48] Quantification was achieved by variable temperature O_2 binding studies (Figures 3a and 3b), which revealed that the earlier report of $[\mathbf{1}]^+$ likely missed superoxide formation because $[\mathbf{1}\cdot O_2]^+$ only appreciably forms below −90 °C. Interestingly, the difference in temperature profiles of O_2 binding between $[\mathbf{1}]^+$ and the N_4-analog $[\mathbf{2}]^+$ was stark (Figures 3b and S3) and could be fit to show dioxygen binding by $[\mathbf{1}]^+$ was more endergonic by $\Delta\Delta H_{[1]-[2]} = +3.2$ kcal/mol and $\Delta\Delta S_{[1]-[2]} = +3.7$ cal/mol·K (see Section 4 in the SI). Cyclic voltammetry showed similar results. Solutions of both $[\mathbf{1}]B(C_6F_5)_4$ and $[\mathbf{2}]B(C_6F_5)_4$ (0.1 mM, 17:3 2-MeTHF/acetone, 0.1 M $TBAPF_6$, 25 °C) exhibited quasi-reversible features and had half-wave potentials at 150 and −126 mV, respectively (Figure 3c; see Figure S4 for CV data in CH_3CN). This corresponds to a 6 kcal/mol difference between Cu^{II}/Cu^{I} reduction potentials, in qualitative agreement with the O_2 binding behavior.

The presence of a cupric superoxide moiety within $[\mathbf{1}\cdot O_2]B(C_6F_5)_4$ was confirmed by resonance Raman (rR) spectroscopic studies on a frozen 2-MeTHF sample (Figure 3d). Laser excitation at 413 nm revealed resonantly enhanced bands at 446 and 1105 cm^{-1} that shifted upon $^{18}O_2$ labeling (425, 1042 cm^{-1}, respectively). The 446 cm^{-1} band can be assigned as the Cu−O stretch and the 1105 cm^{-1} band as the superoxide O−O stretch in line with other η^1-end-on-bound superoxides, including $[\mathbf{2}\cdot O_2]^+$.[26,32,33,45,50−52]

Importantly, this assignment left unresolved the question of a Cu^{II}−S interaction in $[\mathbf{1}\cdot O_2]^+$. To address this, and as previously successfully applied,[41,42] Cu K-edge X-ray absorption spectroscopy (XAS) studies were undertaken on frozen 2-MeTHF solutions of both $[\mathbf{1}]B(C_6F_5)_4$ and $[\mathbf{1}\cdot O_2]B(C_6F_5)_4$ (Figure 3e). An electric dipole-forbidden quadrupole-allowed 1s−3d transition pre-edge feature was observed for $[\mathbf{1}\cdot O_2]^+$ at ∼8979 eV, indicative of significant Cu^{II} character.[53] In contrast, $[\mathbf{1}]^+$ shows an intense feature at ∼8984 eV from the electric dipole-allowed 1s−4p transition expected of Cu^{I} complexes.[54] The absence of this feature in $[\mathbf{1}\cdot O_2]^+$ demonstrates little-to-no residual $[\mathbf{1}]^+$.

The Cu K-edge EXAFS data and corresponding Fourier transforms (FT) provided geometrical insight (Figure 3f). Compared to $[\mathbf{1}]^+$, $[\mathbf{1}\cdot O_2]^+$ exhibits shifts in the EXAFS beat pattern to higher *k* and in the first-shell FT peak to lower *R* (SI Figure S5b), suggesting a general contraction in the first coordination sphere of $[\mathbf{1}\cdot O_2]^+$. Careful fitting revealed this contraction was not uniform (SI Table S2): $[\mathbf{1}]^+$ had 3 Cu−N/O at 2.01 Å and 1 Cu−S at 2.26 Å, while $[\mathbf{1}\cdot O_2]^+$ had 4 Cu−N/O at 1.98 Å and 1 Cu−S at 2.55 Å. Thus, the Cu−S bond lengthened upon O_2 binding. The distances agree with XRD of $[\mathbf{1}]B(C_6F_5)_4$ and related copper−dialkylthioether distances[39,55,56] in the Cambridge Structural Database ($Cu^{I}\cdots S$ 2.24−2.43 Å, $Cu^{II}\cdots S$ 2.30−2.74 Å).[57] The relatively high σ^2 for the Cu−S path of $[\mathbf{1}\cdot O_2]^+$ (SI Table S2) reflects higher disorder, reasonable considering the fairly long interatomic distance. The Cu−S contributions were essential to achieve good fits; fits for $[\mathbf{1}\cdot O_2]^+$ replacing the Cu−S interaction with Cu···C or Cu···O scatterers were poorer, most noticeably in

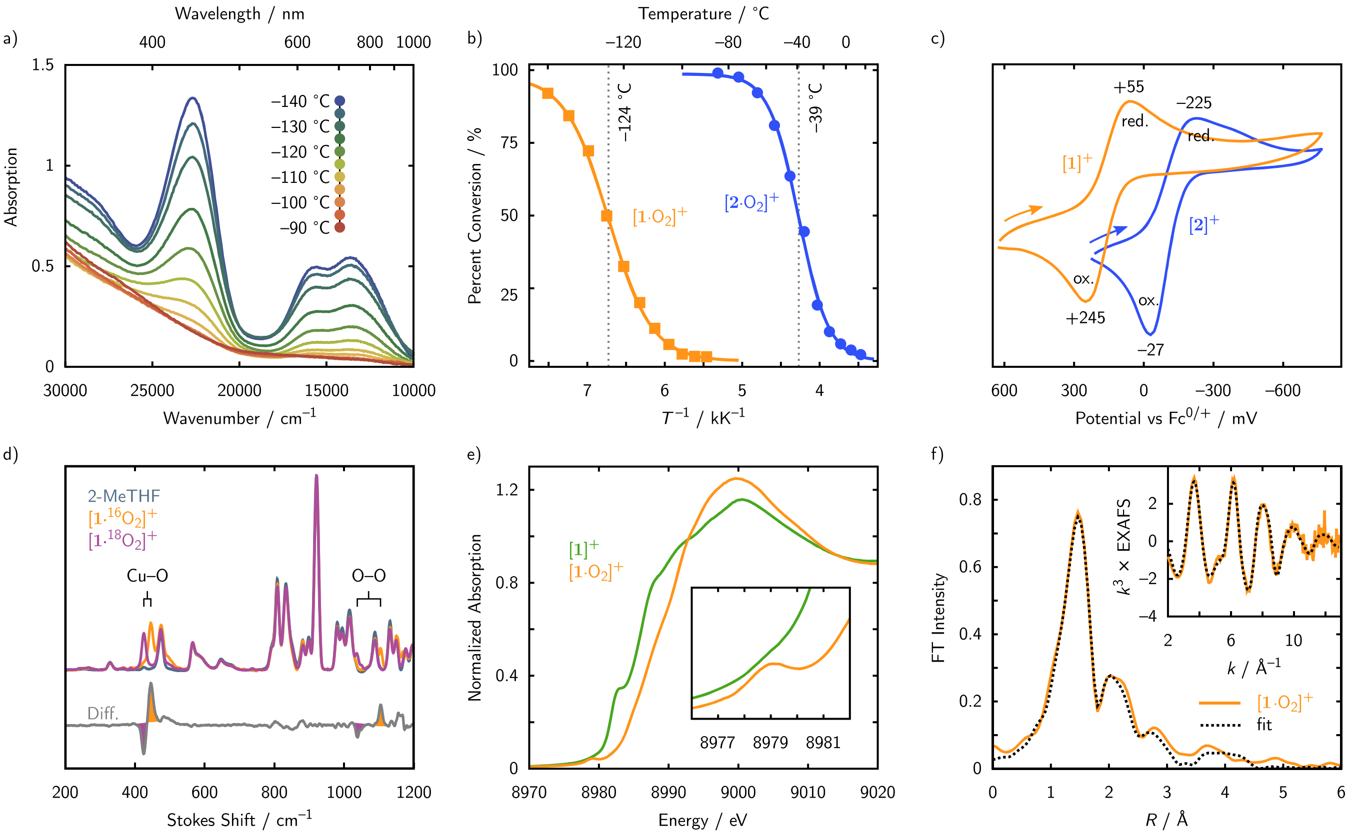

Figure 3. (a) UV/vis spectra show $[\mathbf{1}]B(C_6F_5)_4$ solutions (0.39 mM, 2-MeTHF) under an O_2 atmosphere to reversibly form $[\mathbf{1}{\cdot}O_2]B(C_6F_5)_4$. (b) O_2 binding curves (UV/vis, 740 nm) and fits (see the SI). (c) CVs of $[\mathbf{1}]B(C_6F_5)_4$ and $[\mathbf{2}]B(C_6F_5)_4$ (~1 mM, 17:3 2-MeTHF/Acetone, 0.1 M $TBAPF_6$). (d) Resonance Raman spectra (413 nm, 20 mW) of the ^{16}O and ^{18}O samples, along with a difference spectrum (gray). (e) Cu K-edge XAS spectra of $[\mathbf{1}]B(C_6F_5)_4$ (green) and $[\mathbf{1}{\cdot}O_2]B(C_6F_5)_4$ (orange) with the expanded pre-edge region (inset). (f) Cu K-edge EXAFS data (inset) and nonphase-shift-corrected FT for $[\mathbf{1}{\cdot}O_2]B(C_6F_5)_4$ (data, solid orange; fits, dotted black).

the ~2 Å FT feature and the larger errors (Figure S5e−f and Table S3).

Density functional theory (DFT) computations supported these structural features. Geometry optimizations of $[\mathbf{1}]^+$ and $[\mathbf{1}{\cdot}O_2]^+$ (Figure 2b) with ORCA 4[58] at the B3LYP-D3(BJ)/Def2-TZVP level of theory[59−65] and a tetrahydrofuran conductor-like polarizable continuum model[66] predicted an end-on $CuO_2^{\bullet-}$ triplet with a CuOO angle of 113° and similar lengthening of the Cu−S bond upon O_2 binding (2.32 to 2.50 Å). The calculated thermodynamics of O_2 binding also agreed reasonably with experiment (vide supra), showing $\Delta\Delta H_{[1]-[2]} = +1.3$ kcal/mol and $\Delta\Delta S_{[1]-[2]} = +1.7$ cal/mol·K. The calculated vibrations (Cu−O 378 cm^{-1}, O−O 1173 cm^{-1}) also comport with our Raman assignments.

Beyond its demonstrable Cu^{II}−S interaction, $[\mathbf{1}{\cdot}O_2]B(C_6F_5)_4$ was remarkable for its stability. Monitoring its formation by UV/vis spectroscopy showed no decay or dimerization over 4 h,[32,49] unlike the previously reported cases with sulfur-substituted ligand frameworks. Cycling a solution from −135 °C to +25 °C and back again gave ~95% recovery of $[\mathbf{1}{\cdot}O_2]^+$, illustrating clean and reversible dioxygen binding (see Figure S2).

Such stability enabled further reactivity studies. Hydrogen atom abstraction (HAA) by $[\mathbf{1}{\cdot}O_2]^+$ was probed using 2,2,6,6-tetramethylpiperidin-1-ol (TEMPO−H; Scheme 2).[67] Monitoring the 742 nm band by UV/vis spectroscopy (2-MeTHF, −135 °C) in the presence of excess TEMPO-H[68] (25−200 equiv) revealed $[\mathbf{1}{\cdot}O_2]^+$ to decay isosbestically by pseudo-first-order kinetics (Figure 4), allowing extraction of a second-order rate constant $k_2 = 1.28 \times 10^{-1}$ M^{-1} s^{-1} (see SI Figures S6−S7 and Table S4), to the putative cupric hydroperoxide $[\mathbf{1}{\cdot}OOH]^+$ (330 nm, 400 nm) in >94% yields (see Section 10 in the SI). Deuteration (100−750 equiv of TEMPO−D[69]) slowed the decay of $[\mathbf{1}{\cdot}O_2]^+$ with $k_D = 0.24 \times 10^{-1}$ M^{-1} s^{-1}, revealing a primary kinetic isotope effect (KIE) of $k_H/k_D = 5.4$ (see Figures S8−S9), indicating a rate-limiting HAA process. To probe the effect of $S_{thioether}$ substitution on the HAA reactivity with the O−H bond of TEMPO−H, the rates of the reaction of $[\mathbf{2}{\cdot}O_2]^+$ were reevaluated in 2-MeTHF at −135 °C and contrasted with that of $[\mathbf{1}{\cdot}O_2]^+$.[48] The obtained pseudo-first-order rate constants (k_{obs}) were plotted (see Figures S10−S11 and Table S5) to yield a second-order rate constant $k_2 = 0.82 \times 10^{-1}$ M^{-1} s^{-1} indicating a slightly slower HAA reactivity by $[\mathbf{2}{\cdot}O_2]^+$ (Figure S12). Quantitation of the products of the HAA reaction between $[\mathbf{1}{\cdot}O_2]^+$ and TEMPO−H, i.e., $[\mathbf{1}{\cdot}OOH]^+$ and TEMPO$^\bullet$, was carried out by showing that the

Scheme 2. HAA from TEMPO−H by $[\mathbf{1}{\cdot}O_2]^+$

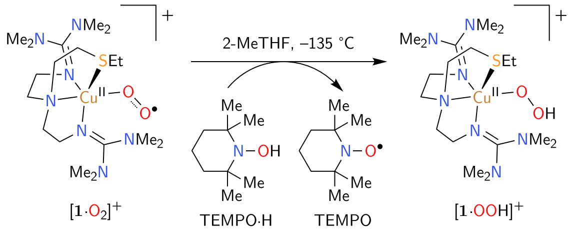

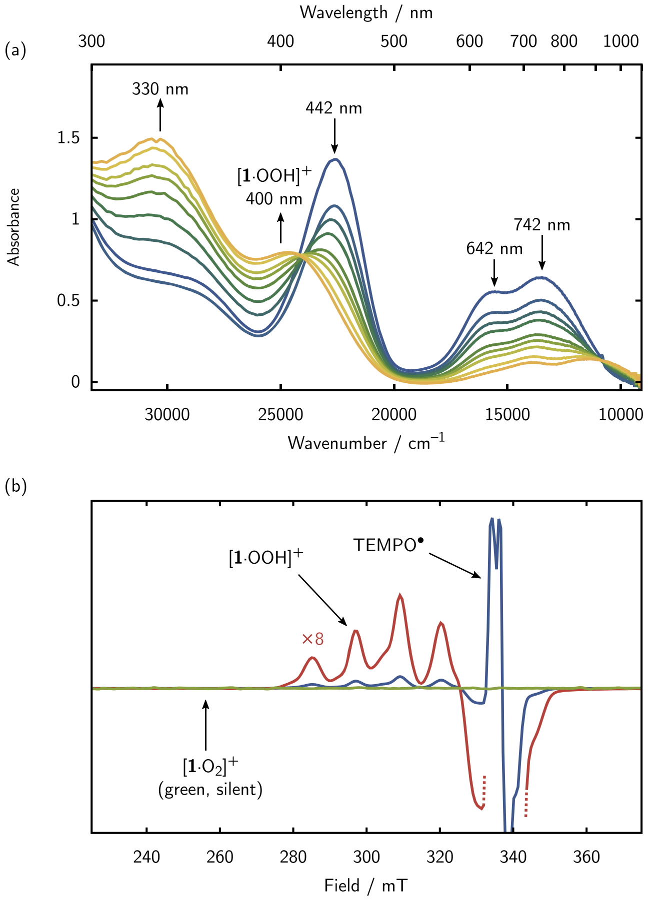

Figure 4. (a) UV/vis (2-MeTHF, −135 °C) and (b) EPR spectroscopic monitoring of the reaction between $[\mathbf{1}\cdot O_2]^+$ and TEMPO−H to generate $[\mathbf{1}\cdot OOH]^+$ and TEMPO$^\bullet$. See Figure S15 for EPR simulation and further discussion.

hydroperoxide $[\mathbf{1}\cdot OOH]^+$ protonates to give H_2O_2 (see Figures S13−S14) and that electron paramagnetic resonance (EPR) spectroscopy reveals the production of Cu^{II} in $[\mathbf{1}\cdot OOH]^+$ along with the TEMPO$^\bullet$ radical in an ~1:1 ratio (see Figure 4 above). These results illustrate that $[\mathbf{1}\cdot O_2]^+$ performs HAA both cleanly and competently. Thus, $[\mathbf{1}\cdot O_2]^+$ is the first thioether Cu_M model to demonstrate Cu_M reactivity.

With this report, we have outlined the stability and reactivity of $[\mathbf{1}\cdot O_2]^+$, the first Cu_M model complex to both unambiguously possess a Cu^{II}−S interaction and perform Cu_M-like HAA. Careful selection of solvent and temperature was crucial to successfully access this superoxide complex. Ongoing research includes studies to obtain deeper insights into the electronic structure of $[\mathbf{1}\cdot O_2]^+$ and their correlation to $[\mathbf{2}\cdot O_2]^+$. This system will be a valuable point of comparison for future work targeting the influence of a sulfur-based ligand in Cu^I/O_2 oxidative reactivity including the methionine residue at the Cu_M active site of noncoupled binuclear copper monooxygenases.

■ ASSOCIATED CONTENT

Supporting Information

The Supporting Information is available free of charge at https://pubs.acs.org/doi/10.1021/jacs.1c00260.

Experimental details, characterization data, and X-ray crystallographic data for $[\mathbf{1}]B(C_6F_5)_4$ (PDF)

Accession Codes

CCDC 2057574 contains the supplementary crystallographic data for this paper. These data can be obtained free of charge via www.ccdc.cam.ac.uk/data_request/cif, or by emailing data_request@ccdc.cam.ac.uk, or by contacting The Cambridge Crystallographic Data Centre, 12 Union Road, Cambridge CB2 1EZ, UK; fax: +44 1223 336033.

■ AUTHOR INFORMATION

Corresponding Authors

Kenneth D. Karlin − *Department of Chemistry, The Johns Hopkins University, Baltimore, Maryland 21218, United States;* orcid.org/0000-0002-5675-7040; Email: karlin@jhu.edu

Edward I. Solomon − *Department of Chemistry, Stanford University, Stanford, California 94305, United States; Stanford Synchrotron Radiation Lightsource, SLAC National Accelerator Laboratory, Stanford University, Menlo Park, California 94025, United States;* orcid.org/0000-0003-0291-3199; Email: edward.solomon@stanford.edu

Authors

Mayukh Bhadra − *Department of Chemistry, The Johns Hopkins University, Baltimore, Maryland 21218, United States;* orcid.org/0000-0002-4758-1610

Wesley J. Transue − *Department of Chemistry, Stanford University, Stanford, California 94305, United States;* orcid.org/0000-0001-7445-5663

Hyeongtaek Lim − *Department of Chemistry, Stanford University, Stanford, California 94305, United States;* orcid.org/0000-0003-3470-8296

Ryan E. Cowley − *Department of Chemistry, Stanford University, Stanford, California 94305, United States;* orcid.org/0000-0003-1791-4266

Jung Yoon C. Lee − *Department of Chemistry, The Johns Hopkins University, Baltimore, Maryland 21218, United States*

Maxime A. Siegler − *Department of Chemistry, The Johns Hopkins University, Baltimore, Maryland 21218, United States;* orcid.org/0000-0003-4165-7810

Patrick Josephs − *Department of Chemistry, University of Paderborn, Paderborn D-33098, Germany*

Gerald Henkel − *Department of Chemistry, University of Paderborn, Paderborn D-33098, Germany*

Markus Lerch − *Institute of Inorganic and Analytical Chemistry, Justus-Liebig University of Gießen, Giessen D-35392, Germany*

Siegfried Schindler − *Institute of Inorganic and Analytical Chemistry, Justus-Liebig University of Gießen, Giessen D-35392, Germany*

Adam Neuba − *Department of Chemistry, University of Paderborn, Paderborn D-33098, Germany*

Keith O. Hodgson − *Department of Chemistry, Stanford University, Stanford, California 94305, United States; Stanford Synchrotron Radiation Lightsource, SLAC National Accelerator Laboratory, Stanford University, Menlo Park, California 94025, United States*

Britt Hedman − *Stanford Synchrotron Radiation Lightsource, SLAC National Accelerator Laboratory, Stanford University, Menlo Park, California 94025, United States*

Complete contact information is available at:
https://pubs.acs.org/10.1021/jacs.1c00260

Notes

The authors declare no competing financial interest.

■ ACKNOWLEDGMENTS

Our research was supported by the U.S. National Institutes of Health (NIH) National Institute of General Medical Sciences (NIGMS) under Awards GM60353 (K.D.K.) and DK31450 (E.I.S.) and the Ruth L. Kirschstein National Research Service Award F32GM131602 (W.J.T.). We acknowledge the use of the Stanford Synchrotron Radiation Lightsource (SSRL), SLAC National Accelerator Laboratory, supported by the U.S. Department of Energy, Office of Science, Office of Basic Energy Sciences under Contract No. DE-AC02-76SF00515. The SSRL Structural Molecular Biology Program is supported by the DOE Office of Biological and Environmental Research, and by the NIH, NIGMS (P30GM133894). Continuous support of the German research council (DFG) and Federal Ministry of education and research (BMBF) is acknowledged. The contents of this publication are solely the responsibility of the authors and do not necessarily represent the official views of the NIGMS or NIH.

■ REFERENCES

(1) Klinman, J. P. Mechanisms Whereby Mononuclear Copper Proteins Functionalize Organic Substrates. *Chem. Rev.* **1996**, *96*, 2541−2562.

(2) Prigge, S. T.; Eipper, B. A.; Mains, R. E.; Amzel, L. M. Dioxygen Binds End-On to Mononuclear Copper in a Precatalytic Enzyme Complex. *Science* **2004**, *304*, 864.

(3) Klinman, J. P. The Copper-Enzyme Family of Dopamine β-Monooxygenase and Peptidylglycine α-Hydroxylating Monooxygenase: Resolving the Chemical Pathway for Substrate Hydroxylation. *J. Biol. Chem.* **2006**, *281*, 3013−3016.

(4) Solomon, E. I.; Heppner, D. E.; Johnston, E. M.; Ginsbach, J. W.; Cirera, J.; Qayyum, M.; Kieber-Emmons, M. T.; Kjaergaard, C. H.; Hadt, R. G.; Tian, L. Copper Active Sites in Biology. *Chem. Rev.* **2014**, *114*, 3659−3853.

(5) Crespo, A.; Martí, M. A.; Roitberg, A. E.; Amzel, L. M.; Estrin, D. A. The Catalytic Mechanism of Peptidylglycine α-Hydroxylating Monooxygenase Investigated by Computer Simulation. *J. Am. Chem. Soc.* **2006**, *128*, 12817−12828.

(6) Yoshizawa, K.; Kihara, N.; Kamachi, T.; Shiota, Y. Catalytic Mechanism of Dopamine β-Monooxygenase Mediated by Cu(III)−oxo. *Inorg. Chem.* **2006**, *45*, 3034−3041.

(7) Abad, E.; Rommel, J. B.; Kaestner, J. Reaction Mechanism of the Bicopper Enzyme Peptidylglycine α-Hydroxylating Monooxygenase. *J. Biol. Chem.* **2014**, *289*, 13726−13738.

(8) Chen, P.; Bell, J.; Eipper, B. A.; Solomon, E. I. Oxygen Activation by the Noncoupled Binuclear Copper Site in Peptidylglycine α-Hydroxylating Monooxygenase. Spectroscopic Definition of the Resting Sites and the Putative $Cu^{II}{}_M$−OOH Intermediate. *Biochemistry* **2004**, *43*, 5735−5747.

(9) Chen, P.; Solomon, E. I. Oxygen Activation by the Noncoupled Binuclear Copper Site in Peptidylglycine α-Hydroxylating Monooxygenase. Reaction Mechanism and Role of the Noncoupled Nature of the Active Site. *J. Am. Chem. Soc.* **2004**, *126*, 4991−5000.

(10) Cowley, R. E.; Tian, L.; Solomon, E. I. Mechanism of O_2 activation and substrate hydroxylation in noncoupled binuclear copper monooxygenases. *Proc. Natl. Acad. Sci. U. S. A.* **2016**, *113*, 12035−12040.

(11) For a recently proposed alternative, see: Wu, P.; Fan, F.; Song, J.; Peng, W.; Liu, J.; Li, C.; Cao, Z.; Wang, B. Theory Demonstrated a "Coupled" Mechanism for O_2 Activation and Substrate Hydroxylation by Binuclear Copper Monooxygenases. *J. Am. Chem. Soc.* **2019**, *141*, 19776−19789.

(12) Cowley, R. E.; Cirera, J.; Qayyum, M. F.; Rokhsana, D.; Hedman, B.; Hodgson, K. O.; Dooley, D. M.; Solomon, E. I. Structure of the Reduced Copper Active Site in Preprocessed Galactose Oxidase: Ligand Tuning for One-Electron O_2 Activation in Cofactor Biogenesis. *J. Am. Chem. Soc.* **2016**, *138*, 13219−13229.

(13) Shepard, E. M.; Dooley, D. M. Inhibition and Oxygen Activation in Copper Amine Oxidases. *Acc. Chem. Res.* **2015**, *48*, 1218−1226.

(14) Johnson, B. J.; Yukl, E. T.; Klema, V. J.; Klinman, J. P.; Wilmot, C. M. Structural Snapshots from the Oxidative Half-reaction of a Copper Amine Oxidase: Implications For O_2 Activation. *J. Biol. Chem.* **2013**, *288*, 28409−28417.

(15) Hess, C. R.; Wu, Z.; Ng, A.; Gray, E. E.; McGuirl, M. A.; Klinman, J. P. Hydroxylase Activity of Met471Cys Tyramine β-Monooxygenase. *J. Am. Chem. Soc.* **2008**, *130*, 11939−11944.

(16) Eipper, B. A.; Quon, A. S.; Mains, R. E.; Boswell, J. S.; Blackburn, N. J. The Catalytic Core of Peptidylglycine α-Hydroxylating Monooxygenase: Investigation by Site-Directed Mutagenesis, Cu X-ray Absorption Spectroscopy, and Electron Paramagnetic Resonance. *Biochemistry* **1995**, *34*, 2857−2865.

(17) Bauman, A. T.; Broers, B. A.; Kline, C. D.; Blackburn, N. J. A Copper−Methionine Interaction Controls the pH-Dependent Activation of Peptidylglycine Monooxygenase. *Biochemistry* **2011**, *50*, 10819−10828.

(18) Hess, C. R.; Klinman, J. P.; Blackburn, N. J. The Copper Centers of Tyramine β-Monooxygenase and its Catalytic-Site Methionine Variants: An X-ray Absorption Study. *JBIC, J. Biol. Inorg. Chem.* **2010**, *15*, 1195−1207.

(19) Blackburn, N. J.; Rhames, F. C.; Ralle, M.; Jaron, S. Major Changes in Copper Coordination Accompany Reduction of Peptidylglycine Monooxygenase: Implications for Electron Transfer and the Catalytic Mechanism. *JBIC, J. Biol. Inorg. Chem.* **2000**, *5*, 341−353.

(20) Schindler, S. Reactivity of Copper(I) Complexes Towards Dioxygen. *Eur. J. Inorg. Chem.* **2000**, *2000*, 2311−2326.

(21) Itoh, S. Developing Mononuclear Copper−Active-Oxygen Complexes Relevant to Reactive Intermediates of Biological Oxidation Reactions. *Acc. Chem. Res.* **2015**, *48*, 2066−2074.

(22) Elwell, C. E.; Gagnon, N. L.; Neisen, B. D.; Dhar, D.; Spaeth, A. D.; Yee, G. M.; Tolman, W. B. Copper−Oxygen Complexes Revisited: Structures, Spectroscopy and Reactivity. *Chem. Rev.* **2017**, *117*, 2059−2107.

(23) Quist, D. A.; Diaz, D. E.; Liu, J. J.; Karlin, K. D. Activation of Dioxygen by Copper Metalloproteins and Insights from Model Complexes. *JBIC, J. Biol. Inorg. Chem.* **2017**, *22*, 253−288.

(24) Noh, H.; Cho, J. Synthesis, Characterization and Reactivity of Non-heme 1st Row Transition Metal-Superoxo Intermediates. *Coord. Chem. Rev.* **2019**, *382*, 126−144.

(25) Fukuzumi, S.; Lee, Y. M.; Nam, W. Structure and Reactivity of the First-row d-block Metal-Superoxo Complexes. *Dalton Trans* **2019**, *48*, 9469−9489.

(26) Maiti, D.; Fry, H. C.; Woertink, J. S.; Vance, M. A.; Solomon, E. I.; Karlin, K. D. A 1:1 Copper−Dioxygen Adduct is an End-on Bound Superoxo Copper (II) Complex which Undergoes Oxygenation Reactions with Phenols. *J. Am. Chem. Soc.* **2007**, *129*, 264−265.

(27) Lee, J. Y.; Peterson, R. L.; Ohkubo, K.; Garcia-Bosch, I.; Himes, R. A.; Woertink, J.; Moore, C. D.; Solomon, E. I.; Fukuzumi, S.; Karlin, K. D. Mechanistic Insights into the Oxidation of Substituted Phenols via Hydrogen Atom Abstraction by a Cupric−Superoxo Complex. *J. Am. Chem. Soc.* **2014**, *136*, 9925−9937.

(28) Würtele, C.; Gaoutchenova, E.; Harms, K.; Holthausen, M. C.; Sundermeyer, J.; Schindler, S. Crystallographic Characterization of a Synthetic 1:1 End-on Copper Dioxygen Adduct Complex. *Angew. Chem., Int. Ed.* **2006**, *45*, 3867−3869.

(29) Fujisawa, K.; Tanaka, M.; Moro-oka, Y.; Kitajima, N. A Monomeric Side-on Superoxo Copper(II) Complex: $Cu(O_2)(HB(3\text{-}{}^tBu\text{-}5\text{-}{}^{iPr}pz)_3)$. *J. Am. Chem. Soc.* **1994**, *116*, 12079−12080.

(30) Kunishita, A.; Kubo, M.; Sugimoto, H.; Ogura, T.; Sato, K.; Takui, T.; Itoh, S. Mononuclear Copper(II)−Superoxo Complexes that Mimic the Structure and Reactivity of the Active Centers of PHM and DβM. *J. Am. Chem. Soc.* **2009**, *131*, 2788−2789.

(31) Zhang, C. X.; Kaderli, S.; Costas, M.; Kim, E.-i.; Neuhold, Y.-M.; Karlin, K. D.; Zuberbühler, A. D. Copper(I)− Dioxygen Reactivity of $[(L)Cu^{I}]^{+}$ (L= Tris (2-pyridylmethyl)amine): Kinetic/Thermodynamic and Spectroscopic Studies Concerning the Formation of $Cu-O_2$ and Cu_2-O_2 Adducts as a Function of Solvent Medium and 4-Pyridyl Ligand Substituent Variations. *Inorg. Chem.* **2003**, *42*, 1807−1824.

(32) Bhadra, M.; Lee, J. Y. C.; Cowley, R. E.; Kim, S.; Siegler, M. A.; Solomon, E. I.; Karlin, K. D. Intramolecular Hydrogen Bonding Enhances Stability and Reactivity of Mononuclear Cupric Superoxide Complexes. *J. Am. Chem. Soc.* **2018**, *140*, 9042−9045.

(33) Diaz, D. E.; Quist, D. A.; Herzog, A. E.; Schaefer, A. W.; Kipouros, I.; Bhadra, M.; Solomon, E. I.; Karlin, K. D. Impact of Intramolecular Hydrogen Bonding on the Reactivity of Cupric Superoxide Complexes with O−H and C−H Substrates. *Angew. Chem., Int. Ed.* **2019**, *58*, 17572−17576.

(34) Kodera, M.; Kita, T.; Miura, I.; Nakayama, N.; Kawata, T.; Kano, K.; Hirota, S. Hydroperoxo−Copper(II) Complex Stabilized by N_3S-Type Ligand Having a Phenyl Thioether. *J. Am. Chem. Soc.* **2001**, *123*, 7715−7716.

(35) Zhou, L.; Nicholas, K. M. Imidazole Substituent Effects on Oxidative Reactivity of Tripodal $(imid)_2(thioether)$ Cu^{I} Complexes. *Inorg. Chem.* **2008**, *47*, 4356−4367.

(36) Aboelella, N. W.; Gherman, B. F.; Hill, L. M.; York, J. T.; Holm, N.; Young, V. G.; Cramer, C. J.; Tolman, W. B. Effects of Thioether Substituents on the O_2 Reactivity of β-Diketiminate−Cu(I) Complexes: Probing the Role of the Methionine Ligand in Copper Monooxygenases. *J. Am. Chem. Soc.* **2006**, *128*, 3445−3458.

(37) Lee, Y.; Lee, D.-H.; Park, G. Y.; Lucas, H. R.; Narducci Sarjeant, A. A.; Kieber-Emmons, M. T.; Vance, M. A.; Milligan, A. E.; Solomon, E. I.; Karlin, K. D. Sulfur Donor Atom Effects on Copper(I)/O_2 Chemistry with Thioanisole Containing Tetradentate N_3S Ligand Leading to μ-1, 2-Peroxo-Dicopper(II) Species. *Inorg. Chem.* **2010**, *49*, 8873−8885.

(38) Martínez-Alanis, P. R.; Sanchez Eguia, B. N.; Ugalde-Saldívar, V. M.; Regla, I.; Demare, P.; Aullón, G.; Castillo, I. Copper Versus Thioether-Centered Oxidation: Mechanistic Insights into the Non-Innocent Redox Behavior of Tripodal Benzimidazolylaminothioether Ligands. *Chem. - Eur. J.* **2013**, *19*, 6067−6079.

(39) Hoppe, T.; Josephs, P.; Kempf, N.; Wölper, C.; Schindler, S.; Neuba, A.; Henkel, G. An Approach to Model the Active Site of Peptidglycine-α-hydroxylating monooxygenase (PHM). *Z. Anorg. Allg. Chem.* **2013**, *639*, 1504−1511.

(40) Tano, T.; Mieda, K.; Sugimoto, H.; Ogura, T.; Itoh, S. A Copper Complex Supported by an N_2S-Tridentate Ligand Inducing Efficient Heterolytic O−O Bond Cleavage of Alkylhydroperoxide. *Dalton Trans* **2014**, *43*, 4871−4877.

(41) Lee, D.-H.; Hatcher, L. Q.; Vance, M. A.; Sarangi, R.; Milligan, A. E.; Narducci Sarjeant, A. A.; Incarvito, C. D.; Rheingold, A. L.; Hodgson, K. O.; Hedman, B.; Solomon, E. I.; Karlin, K. D. Copper(I) Complex O_2-Reactivity with a N_3S Thioether Ligand: a Copper−Dioxygen Adduct Including Sulfur Ligation, Ligand Oxygenation, and Comparisons with All Nitrogen Ligand Analogues. *Inorg. Chem.* **2007**, *46*, 6056−6068.

(42) Hatcher, L. Q.; Lee, D.-H.; Vance, M. A.; Milligan, A. E.; Sarangi, R.; Hodgson, K. O.; Hedman, B.; Solomon, E. I.; Karlin, K. D. Dioxygen Reactivity of a Copper(I) Complex with a N_3S Thioether Chelate; Peroxo−Dicopper(II) Formation Including Sulfur-Ligation. *Inorg. Chem.* **2006**, *45*, 10055−10057.

(43) Park, G. Y.; Lee, Y.; Lee, D.-H.; Woertink, J. S.; Sarjeant, A. A. N.; Solomon, E. I.; Karlin, K. D. Thioether S-ligation in a Side-on μ-η^2:η^2-peroxodicopper(II) complex. *Chem. Commun.* **2010**, *46*, 91−93.

(44) Kim, S.; Ginsbach, J. W.; Billah, A. I.; Siegler, M. A.; Moore, C. D.; Solomon, E. I.; Karlin, K. D. Tuning of the Copper−Thioether Bond in Tetradentate N_3S (thioether) Ligands; O−O Bond Reductive Cleavage via a $[Cu^{II}_2(\mu\text{-1,2-peroxo})]^{2+}/[Cu^{III}_2(\mu\text{-oxo})_2]^{2+}$ Equilibrium. *J. Am. Chem. Soc.* **2014**, *136*, 8063−8071.

(45) Kim, S.; Lee, J. Y.; Cowley, R. E.; Ginsbach, J. W.; Siegler, M. A.; Solomon, E. I.; Karlin, K. D. A N_3S(thioether)-ligated Cu^{II}-superoxo with Enhanced Reactivity. *J. Am. Chem. Soc.* **2015**, *137*, 2796−2799.

(46) Wittmann, H.; Raab, V.; Schorm, A.; Plackmeyer, J.; Sundermeyer, J. Complexes of Manganese, Iron, Zinc, and Molybdenum with a Superbasic Tris (guanidine) Derivative of Tris (2-ethylamino) amine (Tren) as a Tripod Ligand. *Eur. J. Inorg. Chem.* **2001**, *2001*, 1937−1948.

(47) Schatz, M.; Raab, V.; Foxon, S. P.; Brehm, G.; Schneider, S.; Reiher, M.; Holthausen, M. C.; Sundermeyer, J.; Schindler, S. Combined Spectroscopic and Theoretical Evidence for a Persistent End-On Copper Superoxo Complex. *Angew. Chem., Int. Ed.* **2004**, *43*, 4360−4363.

(48) Maiti, D.; Lee, D. H.; Gaoutchenova, K.; Würtele, C.; Holthausen, M. C.; Narducci Sarjeant, A. A.; Sundermeyer, J.; Schindler, S.; Karlin, K. D. Reactions of a Copper(II) Superoxo Complex Lead to C−H and O−H Substrate Oxygenation: Modeling Copper-Monooxygenase C−H Hydroxylation. *Angew. Chem., Int. Ed.* **2008**, *47*, 82−85.

(49) Karlin, K. D.; Wei, N.; Jung, B.; Kaderli, S.; Zuberbuehler, A. D. Kinetic, Thermodynamic, and Spectral Characterization of the Primary Copper-Oxygen ($Cu-O_2$) Adduct in a Reversibly Formed and Structurally Characterized Peroxo-dicopper(II) Complex. *J. Am. Chem. Soc.* **1991**, *113*, 5868−5870.

(50) Peterson, R. L.; Himes, R. A.; Kotani, H.; Suenobu, T.; Tian, L.; Siegler, M. A.; Solomon, E. I.; Fukuzumi, S.; Karlin, K. D. Cupric Superoxo-Mediated Intermolecular C−H Activation Chemistry. *J. Am. Chem. Soc.* **2011**, *133*, 1702−1705.

(51) Woertink, J. S.; Tian, L.; Maiti, D.; Lucas, H. R.; Himes, R. A.; Karlin, K. D.; Neese, F.; Würtele, C.; Holthausen, M. C.; Bill, E.; Sundermeyer, J.; Schindler, S.; Solomon, E. I. Spectroscopic and Computational Studies of an End-on Bound Superoxo-Cu(II) Complex: Geometric and Electronic Factors That Determine the Ground State. *Inorg. Chem.* **2010**, *49*, 9450−9459.

(52) Peterson, R. L.; Ginsbach, J. W.; Cowley, R. E.; Qayyum, M. F.; Himes, R. A.; Siegler, M. A.; Moore, C. D.; Hedman, B.; Hodgson, K. O.; Fukuzumi, S.; Solomon, E. I.; Karlin, K. D. Stepwise Protonation and Electron-Transfer Reduction of a Primary Copper−Dioxygen Adduct. *J. Am. Chem. Soc.* **2013**, *135*, 16454−16467.

(53) DuBois, J. L.; Mukherjee, P.; Stack, T. D. P.; Hedman, B.; Solomon, E. I.; Hodgson, K. O. A Systematic K-edge X-ray Absorption Spectroscopic Study of Cu(III) Sites. *J. Am. Chem. Soc.* **2000**, *122*, 5775−5787.

(54) Kau, L. S.; Spira-Solomon, D. J.; Penner-Hahn, J. E.; Hodgson, K. O.; Solomon, E. I. X-ray Absorption Edge Determination of the Oxidation State and Coordination Number of Copper. Application to the Type3 Site in Rhus vernicifera Laccase and its Reaction with Oxygen. *J. Am. Chem. Soc.* **1987**, *109*, 6433−6442.

(55) Flörke, U.; Josephs, P. *CCDC 1846820*; Experimental Crystal Structure Determination, 2018, DOI: 10.5517/ccdc.csd.cc1zzrvk.

(56) Flörke, U.; Josephs, P. *CCDC 1846881*; Experimental Crystal Structure Determination, 2018, DOI: 10.5517/ccdc.csd.cc1zzttl.

(57) Groom, C. R.; Bruno, I. J.; Lightfoot, M. P.; Ward, S. C. The Cambridge Structural Database. *Acta Crystallogr., Sect. B: Struct. Sci., Cryst. Eng. Mater.* **2016**, *72*, 171−179.

(58) Neese, F. Software update: the ORCA program system, version 4.0. *WIREs Comput. Mol. Sci.* **2018**, *8*, No. e1327.

(59) Becke, A. D. Density-functional Exchange-energy Approximation with Correct Asymptotic Behavior. *Phys. Rev. A: At., Mol., Opt. Phys.* **1988**, *38*, 3098−3100.

(60) Lee, C.; Yang, W.; Parr, R. G. Development of the Colle-Salvetti Correlation-energy Formula into a Functional of the Electron Density. *Phys. Rev. B: Condens. Matter Mater. Phys.* **1988**, *37*, 785−789.

(61) Grimme, S.; Ehrlich, S.; Goerigk, L. Effect of the Damping Function in Dispersion Corrected Density Functional Theory. *J. Comput. Chem.* **2011**, *32*, 1456−1465.

(62) Grimme, S.; Antony, J.; Ehrlich, S.; Krieg, H. A Consistent and Accurate ab initio Parametrization of Density Functional Dispersion

Correction (DFT-D) for the 94 Elements H-Pu. *J. Chem. Phys.* **2010**, *132*, 154104.

(63) Weigend, F.; Ahlrichs, R. Balanced Basis Sets of Split Valence, Triple Zeta Valence and Quadruple Zeta Valence Quality for H to Rn: Design and Assessment of Accuracy. *Phys. Chem. Chem. Phys.* **2005**, *7*, 3297−3305.

(64) Neese, F.; Wennmohs, F.; Hansen, A.; Becker, U. Efficient, Approximate and Parallel Hartree-Fock and Hybrid DFT Calculations. A 'Chain-of-Spheres' Algorithm for the Hartree-Fock Exchange. *Chem. Phys.* **2009**, *356*, 98.

(65) Weigend, F. Accurate Coulomb-fitting Basis Sets for H to Rn. *Phys. Chem. Chem. Phys.* **2006**, *8*, 1057−1065.

(66) Barone, V.; Cossi, M. Quantum Calculation of Molecular Energies and Energy Gradients in Solution by a Conductor Solvent Model. *J. Phys. Chem. A* **1998**, *102*, 1995−2001.

(67) Warren, J. J.; Tronic, T. A.; Mayer, J. M. Thermochemistry of Proton-Coupled Electron Transfer Reagents and its Implications. *Chem. Rev.* **2010**, *110*, 6961−7001.

(68) Mader, E. A.; Davidson, E. R.; Mayer, J. M. Large Ground-State Entropy Changes for Hydrogen Atom Transfer Reactions of Iron Complexes. *J. Am. Chem. Soc.* **2007**, *129*, 5153−5166.

(69) Wu, A.; Mader, E. A.; Datta, A.; Hrovat, D. A.; Borden, W. T.; Mayer, J. M. Nitroxyl Radical Plus Hydroxylamine Pseudo Self-Exchange Reactions: Tunneling in Hydrogen Atom Transfer. *J. Am. Chem. Soc.* **2009**, *131*, 11985−11997.